Production of xylooligosaccharides, bioethanol, and lignin from structural components of barley straw pretreated with a steam explosion

Álvarez, Cristina*, González, Alberto, Ballesteros, Ignacio, Negro, María José.

Advanced Biofuels and Bioproducts Unit, Renewable Energies Department, CIEMAT, Madrid, 28040, Spain

*Corresponding author E-mail: cristina.alvarez@ciemat.es

Production of xylooligosaccharides, bioethanol, and lignin from structural components of barley straw pretreated with a steam explosion

Álvarez, Cristina*, González, Alberto, Ballesteros, Ignacio, Negro, María José.

Advanced Biofuels and Bioproducts Unit, Renewable Energies Department, CIEMAT, Madrid, 28040, Spain

Corresponding author: Álvarez, C. Phone: 0034913466057. E-mail: cristina.alvarez@ciemat.es

Abstract

Barley straw (BS) is a potential source to obtain bioethanol and value-added products such as xylooligosaccharides (XOS) and lignin for application in diverse industries. In this study, BS was submitted to steam explosion pretreatment to valorize the main components of this lignocellulose biomass. For hemicellulose fraction valorization, different combinations of endo-β-(1,4)-D-xylanase enzyme with accessory enzymes (α-L-arabinofuranosidase, feruloy -esterase and acetylxylan-esterase) have been studied to produce XOS with a low degree of polymerization. The application of accessory enzymes combined with endo-β-(1,4)-D-xylanase enzymes turned out to be the most effective strategy for the formation of XOS. The solid fraction obtained after the pretreatment was submitted to presacharification and simultaneous saccharification and fermentation process for bioethanol production. The resulting lignin-rich residue was characterized. In this integrated process, 13.0 g XOS (DP2-DP6), 12.6 g ethanol and 16.6 g lignin were obtained from 100 g of BS, achieving the goal of valorizing this agricultural residue.

Keywords: lignin, bioethanol, bio-refinery, enzymatic hydrolysis, xylooligosaccharides

1. Introduction

The hemicellulose is the second polymer more abundant in the plant cell wall. This term describes diverse heteropolysaccharides, with a variable structure formed of hexoses (D-glucose, D-galactose and D-mannose) and pentose (D-xylose and L-arabinose) (Limayem and Ricke, 2012). The hemicelluloses are classified according to the main residues of sugars present in the backbone of the structural polymer, being xylan is the main hemicellulose in herbaceous plants and hardwoods. In gramineous plants, the xylans are made up of the main backbone of xylose units linked by β-1,4 bonds which, shows a great variety of linkages and branching by functional groups such as acetyl, methyl, cinnamic acids (*p*-coumaric or ferulic acid) or glucuronic acids (Gírio et al., 2010). These functional groups usually covalently linked between arabinofuranosyl residues whereas, *p*-coumaric or ferulic acids are joined through an ester linkage.

The hemicellulose polymers are interconnected by covalent and hydrogen bonds with other polymers present in lignocellulosic biomass. Via hydrogen bonds, the hemicellulose chains are bound to cellulose and aromatic esters to lignin, joining the bond between cellulose and lignin (Houfani et al., 2020). For accessing carbohydrates, the lignocellulosic biomass must undergo fractionation steps to overcome these forces and thus utilise the main constituents to carry out individualised processing.

The pretreatment approach related to hemicellulose is dependent on the final application of hemicellulose. Thus, on this occasion, the steam explosion (SE) method was employed to alter the structure of the lignocellulose biomass. For biomass such as agro-industrial waste, this pretreatment is one of the most excellent for disturbed the structure (Moreno et al., 2019). The feedstock is subjected to high temperature at

saturated steam (> 160ºC) during a period of time before sudden depressurisation. In these conditions; it is produce to hydrolysis of acetyl groups present in the hemicellulose generated acetic acids leading to a greather hydrolyze hemicelluloses (Duque et al., 2016).

From hemicellulose fraction in the biorefinery context, high added value products can be obtained to be applied in many manufactures such as pharmaceutical, food or energy. In this context, xylooligosaccharides (XOS) are an interesting compound because they belong to the so-called emerging prebiotics. Prebiotics are defined as "a substrate that is selectively utilised by host microorganisms conferring a health benefit" (Gibson et al., 2017). These compounds have many potential applications in the cosmetic, chemical, or pharmaceutical (Gibson et al., 2017). It is estimated that the prebiotic market will impact 9.5 billion by 2027 (Ahuja and Mamtani, 2021).

XOS with a low degree of polymerization presents several biological benefits; they can improve the immunomodulatory functions, antiinflammatory properties, blood sugar reducer and antioxidant activity (Fernández et al., 2016; Gibson et al., 2017; Pinales-Márquez et al., 2021; Slavin, 2013). These biological activities can be affected by molecular weight, distributions, substitutions of XOS or the source and process used for obtaining it (Zhang et al., 2018).

In the literature, many lignocellulosic residues have been studied to obtain XOS. Agricultural residues are a promising feedstock for emerging bioeconomic concept (Wietschel et al., 2019). Different lignocellulosic biomasses are explored in the production of XOS, such as chestnut shells, wheat straw or peanut shells (Gullón et al., 2018; Pinales-Márquez et al., 2021; Rico et al., 2018). Among lignocellulosic materials, barley straw (BS) is an interesting residue that can be transformed on by-products

interested in many industries. The bioeconomic forecast potential from barley straw has been estimated as 18 million tons in 2030. This estimation is based on considering competing applications of straw (beeding animals, other agricultural uses and mushroom cultivation) (Wietschel et al., 2019).

The XOS can be produced mainly by different strategies, chemical and hydrothermal pretreatment, enzymatic hydrolysis (EH) or a combination of pretreatment and EH (Arai et al., 2019; Gullón et al., 2018; Huang et al., 2017; Rico et al., 2018). In EH process are used a xylanolytic enzyme system, which is generally formed of the repertoire of hydrolytic enzymes such as endo-β-(1,4)-D-xylanase, β-xylosidase, α-L-arabinofuranosidase, acetylxylan esterase, and α-D-glucuronidase. The use of xylanolytic enzymatic allows several advantages such as higher yields, mild reaction conditions and no generation of by-products when as compared with the others process (Sadaf and Khare, 2014). To obtain XOS with low degree of polymerization (DP2-DP6), various hydrolytic enzymes are required with different activities, which release the side-chain substitution, achieving major depolymerisation of xylan.

The production of ethanol from lignocellulosic biomass based on the use of enzymes followed by fermentation is considered a promising technology in biochemical platforms. Bioethanol production from agriculture residue produces a residue rich in lignin, which can be transformed into surfactants/dispersant additives or aromatic compounds (Santos et al., 2015). Typically other application of this residue is used as an energy resource (Sannigrahi and Ragauskas, 2011).

The main goal of this investigation was to study the behavior of several enzymes with accessory activities for increases the production of XOS using SE to solubilize the hemicellulose from barley straw. Also, a brief preliminary study of the integration of

bioethanol production from sugars and energy generation from the rich lignin residue of barley straw is presented.

2. Material and methods

2.1. Raw material and pretreatment

Barley straw (10% moisture) was provided by CEDER (Centro de Desarrollo de Energías Renovables, Spain). The biomass composition was determined according to the NREL procedures (Sluiter et al., 2010). BS (6-10 mm) was pretreated by the steam explosion in a 10 L reactor at 180 ºC for 30 min in a small prototype plant (CIEMAT, Spain). The reactor was preheated at the set pretreatment temperature with saturated steam. After biomass addition into the reactor, it took less than 60 seconds to reach working temperature. The pressure necessary to reach the temperature was 10 bar. These conditions were chosen as such compromise conditions to recover more amounts of cellulose and hemicellulose as possible. After the steam explosion pretreatment, the material (slurry) was recovered, cooled and filtered to separate insoluble solids and the liquid fraction. The solid fraction were thoroughly washed obtaining the water insoluble solids fraction (WIS). The liquid fraction can contain degradation compounds from sugar and derivates lignin, were removed using a cleaning step with ion exchange resin (Microionex MB200 resin (Rohm-Hass Copenhagen, Denmark), following the method Negro et al. (2014) giving rise to a sample called liquid fraction of barley straw pretreated (*Lfbsp*). The liquid from the steam explosion pretreatment, free of degradation compounds, will be called the degradation compounds will be referred to as the liquid fraction of pretreated barley straw (Lfpbs), and will be the starting substrate to obtain the low polymerization degree xylooligosaccharides.

120 **2.2. Enzymatic hydrolysis of the liquid fraction of barley straw pretreated**

121 A series of enzymes with different activities were chosen to obtain XOS with
122 (DP2-DP6) from the *Lfbsp*. Two Commercial endo-β-(1,4)-D-xylanase M1 (E-XYTRI
123 M1 GH11) from Megazyme International (Bray, Ireland) and *NS50030* from
124 Novozymes AS, (Bagsværd, Denmark), were used. In addition, accessory enzymes that
125 are able to hydrolysate linkages among xylan chain and substituent residues such as α-L-
126 arabinofuranosidase (E-AFASE, GH51), feruloyl esterase (E-FAEZCT, CE1), and
127 acetylxylan esterase (E-AXEAO-IKU, CE6) from Megazyme International (Bray,
128 Ireland) were tested. Enzyme loadings for the several tests were following: *Endo-β-*
129 *(1,4)-D-xylanase* M1 5 U/mL; *Endo-β-(1,4)-D-xylanase NS50030* 7.2 U/mL ;α-L-
130 arabinofuranosidase 6.3 U/mL; feruloyl esterase 0.05 U/mL, and acetylxylan esterase 5
131 U/mL. The reactions were stopped by boiling at 100ºC for 5 minutes before being
132 analysed. The reaction conditions were the following pH 4.8 and 50ºC (0.05 M sodium
133 citrate buffer) in an incubator shaker at 150 rpm (Infors HT Minitron Bottmingen,
134 Switzerland).

135 **2.3. Presaccharification simultaneous saccharification and fermentation process**
136 **(PSSF) of WIS**

137 A PSSF process was carried out as previously described Álvarez et al. (2018).
138 Briefly, the pre-hydrolysis stage (8 h at 50ºC) was performed using the WIS obtained
139 after pretreatment at a solids concentration of 20% (w/v) and an enzyme load (Cellic
140 CTec2 Sigma Aldrich USA) of 30 FPU/g glucan. The fermentation stage was carried out
141 at 35ºC using *Saccharomyces cerevisiae* Ethanol Red (inoculum size 0.25 g/L). After 48
142 h of process, the resulting residue was washed with water and dried at 60ºC, determining
143 the content of carbohydrates and lignin (Sannigrahi and Ragauskas, 2011) .

2.4. Analytical methods

2.4.1. Characterization of raw material, WIS and lignin-rich residue

The chemical composition of raw material, WIS and the lignin-rich residue was determined using the method described by Sluiter et al. (2010).

Additionally, in the lignin-rich residue, the ultimate analysis was measured by using LECO TRUSPEC analyser, following the procedure based on ISO 1648. Calorific value was determined by utilizing a LECO AC500 bomb calorimeter.

2.4.2. Sugar (oligomers and monomers), furans, phenolic compounds and organic acids

As the sugars (monomeric and oligomeric form), such as sugar degradation compounds included furfural and 5- hydroxymethylfurfural (HMF), phenolic compounds (ferulic and *p*- coumaric acids) from lignin released during pretreatment and acetic acid were analysed and quantified by high-performance liquid chromatography HPLC following the methodology described in Álvarez et al. (2017).

2.4.3. Xylooligosaccharides analysis

XOS X_2, X_3, X_4, X_5 and X_6 (xylobiose, xylotriose, xylotetraose, xylopentose and xylohexose, respectively) generated in the process were quantified by High performance anion-exchange chromatography ICS2500 Dionex System (Dionex Corporation, Sunnyvale, CA) with a pulsed amperometric detector (ED50 electrochemical detector) with a gold electrode using Dionex CarboPac PA100 analytical column and PA100 guard-column. The sample were eluated with a linear gradient program from 100% A (NaOH 100 mM) to 30% B (NaOAc 500 mM/NaOH 100 mM) and at flow rate of 0.6 mL/min.

2.4.4. Fourier Transformed Infrared Radiation analysis

FTIR spectra Fourier Transformed Infrared Radiation (FTIR) spectra were measured in a Nicolet (Thermo Fisher Scientific) Nexus spectrometer equipped with a Smart Golden Gate ATR (Thermo Electron Scientific Instruments LLC, Madison, WI USA) accessory attenuated total reflectance device. Spectra were collected in the 400-600 cm^{-1} range with a 0.25 cm^{-1} resolution and an average of 64 scans. This technique was used for the characterization of lignin-rich residue.

3. Results and discussion

3.1. Characterisation of raw material and fractions obtained after pretreatment

Cellulose, hemicellulose, and acid insoluble lignin content on barley straw represent 32.9%, 27.2%, and 16.8% dry matter content, respectively (Fig. 1). The majority component of hemicellulose was xylan (22.1%), and minor proportions were determined as arabinans (3.6%), galactans (1.3%), and mannans (0.3%). Acetyl groups account for 1.7%. Although there are slight variations, due to various factors such as the variety of barley, soil composition, climate or type and amount of fertilisers used, and also the method of chemical composition characterisation, the barley composition is in the range of those determined by other authors, 32-40% in cellulose, 21-27% in hemicellulose and 15-22% in lignin (Duque et al., 2014b, 2014a; Lara-Serrano et al., 2018; Sáez et al., 2013). Above 60% of compounds present in the lignocellulosic material of BS are carbohydrates, an excellent material for sugars production and conversion to ethanol, and high added-value products such as producing XOS (DP2-DP6). It is an appropriate substrate to be used in biorefineries.

190 The compositions of solid obtained after pretreated are depited in figure 1. This
191 fraction contained a higher proportion of cellulose (55.8%), and lignin (30.7%) than raw
192 material (Fig. 1). Pretreatment increased the cellulose proportion of WIS due to the
193 extensive solubilisation of the hemicellulose fraction. Hemicellulose content was 10.3%.

194 ***Fig 1.***

195 In liquid fraction, sugars were determined as monomeric and oligomeric form,
196 being the xylose (monomeric form, 3.1 g/L as oligomeric form 25.3 g/L) the main sugar,
197 followed of glucose (0.9 and 5.2 g/L, and minor amounts galactose 1.6 and 0.6 g/L,
198 arabinose 1.2 and 2.1 g/L and mannose 0.4 and 0.07 g/L such monomeric and
199 oligomeric form respectively.

200 During pretreatment, in addition to solubilising the hemicellulosic-derived
201 sugars, acetyl groups were also released from hemicellulose in the form of acetic acid
202 (1.7 g/L). Also, a small concentration of compounds derived from lignin such as vanillin
203 (4-hydroxy-3- methoxybenzaldehyde) (40.5 mg/L) from the release of guayacyl propane
204 units, and ferulic acid (34.5 mg/L), and *p*-coumaric acid (30 mg/L) compounds that are
205 part of the group of hydroxycinnamic acids were detected. Finally, degradation products
206 such as furfural and HMF (0.9 and 0.1 g/L) had also been identified, respectively.

207 Liquid fraction (hydrolysate) contained soluble hemicellulose to obtain high-
208 added value compounds, such as prebiotic xylooligosaccharides. Most of the
209 degradation compounds (furfural, HMF), acetic and formic acids and phenolic
210 compounds generated during pretreatment were removed using an ion exchange resin as
211 cleaning step. The sugars value was not affected by the cleaning step. However, the
212 concentration of furans compounds were reduced up to 0.22 and 0.02 g/L furfural and HMF

213 respectively, while those carboxylic acids were eliminated. This step is necessary because
214 these degradation compounds may hinder enzymatic hydrolysis. *Lfbsp* presented an
215 oligosaccharides concentration of 31.7 g/L, of which 25.3 g/L are xylooligosaccharides.
216 These values refer to raw material are equivalent to 17.5 g oligosaccharides/100 g barley
217 straw and 13.9 g XOS/100 g BS.

218 XOS (DP2-DP6) profile present in the *Lfbsp* is X_2 (2.8 g/L), X_3 (2.5 g/L), X_4 (2.8
219 g/L), X_5 (2.7 g/L), and X_6 (2.4 g/L) and account for 7.9 g/100 g of raw material. Several
220 enzymes with different activities (endo-β-(1,4)-D-xylanase, α-L-arabinofuranosidase,
221 acetylxylan esterase and feruloyl esterase) has been studied in order to achieve the
222 depolymerisation of xylan chains present in the liquid fraction. This set of enzymes
223 forms an enzymatic cocktail. The advantage of using an enzymatic cocktail consortium
224 is that it acts on the terminal and/or internal glucosidic linkages; each enzyme can act on
225 different bonds present in the polymers.

226 **3.2. Enzymatic hydrolysis of barley straw pretreated for production of XOS**

227 In previous work carried out, it has chosen of the pure endo-β-(1,4)-D-xylanase
228 M1 (GH11) from *Trichoderma viride* as the endoxylanase that more amount of XOS
229 produce from barley straw pretreated in front endo-β-(1,4)-D-xylanase from *Thermotoga*
230 *maritima* GH10 (Álvarez et al., 2018).

231 In order to progress the research, the next step was to add accessory enzymes for
232 hydrolysis of hemicellulose. In this section, the results achieved in the experiments carry
233 out with the combination of enzymes were showed. Four different enzymes formulations
234 were evaluated for increased XOS from BS pretreated.

235 ***3.2.1. Enzymatic hydrolysis employing endo-β-(1,4)-D-xylanase (M1), α-L-***
236 ***arabinofuranosidase, and feruloyl esterase***

237 The first cocktail of the enzyme used was called *Maf*. This cocktail is composed of
238 endo-β-(1,4)-D-xylanase (M1), α-L-arabinofuranosidase, and feruloyl esterase. The
239 goals of this enzymatic hydrolysis are *i)* help hydrolysis of xylanase, a obtain XOS of
240 low degree of polymerisation and *ii)* reduce the substitutes presents in XOS since as
241 more lineal is XOS easier fermentable will be for bifidobacteria (Vazquez-Olivo et al.,
242 2019).

243 The efficiency of enzymatic hydrolysis can be reduced through arabinoxylan with
244 ferulic acid cross-linking (de Oliveira et al., 2015). In this context, the synergy action of
245 feruloyl esterase has been demonstrated with endo-β-(1,4)-D-xylanase) and α-L-
246 arabinofuranosidase, among others in the degradation of plant cell walls. This fact
247 supposes a reduction of the enzyme dosage, consequently impacting the prices of the
248 final products. The concentration of cinnamic acids (ferulic acid and *p*-coumaric) was
249 monitoring during EH trial. The maximum value of the concentration of ferulic and *p*-
250 coumaric acid (96 and 29 mg/L respectively) was achieved in a short time of hydrolysis
251 (1 h of reaction). From this time on, the concentrations remained constant. The
252 production of ferulic and *p*-coumaric acids is because the enzyme feruloyl esterase can
253 hydrolysing the ester linkage (Wong et al., 2013).

254 In addition, the production of low DP XOS was monitored over reaction time
255 (Fig. 2a). The XOS majority was xylobiose, whose maximum value is 13.6 g/L at 5 h.
256 This concentration supposes 48.8% of potential xylose present as oligosaccharide in the
257 liquid fraction of barley straw pretreated. The maximum amounts of X_2, X_3, X_4, X_5 and
258 X_6 were 12.5; 3.5; 2.6; 1.4; and 0.7 g/L, respectively. These values were achieved at 4 h
259 of reaction, and these data have shown the ability of the enzyme cocktail to produce
260 mainly short-chain XOS (xylobiose and xylotriose). A similar trend was observed by

Avila et al. (2020b) in the hydrolysis of extracted xylan from sugarcane straw and coffee husk by a mixture of endo-β-(1,4)-D-xylanase, α-L-arabinofuranosidase, and feruloyl esterase. XOS with a low degree of polymerisation are easily metabolised by probiotic bacteria, being these types of XOS preferred for food applications industries (Reddy and Krishnan, 2016).

Fig. 2.

Concerning arabinose production, the release of arabinose (0.4 g/L) was due to the action of α-L-arabinofuranosidase together with feruloyl esterase because some arabinofuranosyl residues are esterified at position 5 with ferulic acid (Biely et al., 2016). Despite this, 65.8% of arabinose continues to link to the soluble hemicellulose. This fact, of the incomplete release of arabinose, could present other substituents such as acetyl groups present in the hemicellulose. These groups can be hampering the action of enzymes.

In this assay, 12.3 g de XOS (DP2-DP6) per 100 g of BS was obtained, meaning an increase of 56% concerning *Lfbsp*.

3.2.2. Enzymatic hydrolysis employing endo-β-(1,4)-D-xylanase (M1), α-L-arabinofuranosidase, acetylxylan esterase and feruloyl esterase

The presence of acetyl groups in the oligosaccharides present in the liquid fraction of BS pretreated was confirmed through techniques FTIR and Matrix-Assisted Laser Desorption/Ionization-Time of Flight-Mass Spectrum in previous work (Álvarez et al., 2020). Thus, acetylxylan esterase enzyme was added to a before cocktail enzymatic, refer to *Complex* cocktail to increase the production of XOS (DP2-DP6). Acetylxylan esterases present a synergistic action with GH10 and GH11 xylanases (Zheng et al.,

2013). The acetyl groups present in the hemicellulose hampered the action of endo-β-(1,4)-D-xylanase enzymes limiting the degree of hydrolysis.

The SE pretreatment was not able to fully be released acetyl groups present in the hemicellulose. In the depolymerisation of solubilised xylan, the acetylxylan esterases enzymes liberate acetic acid, esterifying D-xylopyranosyl residue. The yield of acetic acid production was relatively low (33.7%), even though the incorporation of acetylxylan esterase. The incomplete deacetylation that occurred in this assay can explain several hypotheses. The experiment was carried out in a compromise condition pH (4.8) for an enzymatic cocktail. This pH is very different from the optimum pH for acetyl esterase (pH 7). This fact can be reduced the mode of the act of acetyl esterase. Another theory for just the low deacetylation can be due to steric hindrance. The literature describes the existence of oligosaccharides with acetylated resistant groups, in particular acetyl groups located on non-reducing-end xylopyranosyl residues that may become non-hydrolysable by spontaneous migration from position 2 and 3 towards position 4 so that total deacetylation does not occur (Biely et al., 2013).

In this test, the maximum release of cinnamic acids (ferulic and *p*-coumaric acids) occurred at short reaction times (1 h). With the *Complex* enzymatic combination, the release has been somewhat lower, obtaining maximum values of 88 and 22 mg/L of ferulic and *p*-coumaric acids, respectively, and this fact could be attributed to the impediment that the presence of the four enzymes could produce. Wu et al. (2017) observed a limited action of feruloyl esterase when increasing the concentration of endo-β-(1,4)-D-xylanase since that the xylan substituents prevent hydrolysis.

Figure 2b illustrates the production profile of different XOS (X_2, X_3, X_4, X_5, and X_6) obtained using the *Complex* as an enzymatic cocktail. During the enzymatic

hydrolysis, a significant concentration of XOS (DP2-DP6) was produced at brief reaction times (45 minutes). After this time, xylose and xylobiose concentrations were increased to a value of 4.5 and 13.7 g/L, respectively, at 5 h. This increase is principally due to a decline in XOS with DP3, DP4, DP5, and DP6 present in the medium. This fact was produced because eliminating the acetyl groups increases the areas in which the enzyme can act by releasing XOS of a low degree of polymerisation (Zhang et al., 2011). The concentration of X_3 was increased to 6.6 g/L at 45 minutes of EH, from which it decreases up to a value of 3.8 g/L. In the case of xylotetraose and xylopentose, the behaviour was similar. The maximum concentration was achieved a brief time (45 minutes), for later decreasing in favour of XOS with a minor degree of polymerisation. In the case of xylohexose was hydrolysed from the beginning of the reaction to a value of 0.1 g/L.

The side chains may influence the rate of hydrolysis of xylan (Brienzo et al., 2016); in this case, the hydrolysis is faster due to the presence of hemicellulose, accessory enzymes acting on the backbone branches.

Given these conditions, 13.0 g of XOS (expressed in xylose form) with DP2-DP6 per 100 g of BS were produced. In this case, an incremented of 64% concerning *Lfbsp* was achieved.

3.2.3. Enzymatic hydrolysis using a commercial endo-β-(1,4)-D-xylanase

Since supplementation with accessory enzymes to hydrolysis with pure commercial endo-β-(1,4)-D-xylanase has recovered high depolymerisation of the pre-hydrolysate, favouring of increased XOS formation, EH experiments have been carried out with an endo-β-(1,4)-D-xylanases commercial enzyme (*NS50030)*. This enzyme

331 presents various activies such as β-xylosidase, α-L-arabinofuranosidase, endo-glucanase,
332 among others.

333 The action of endo-β-(1,4)-D-xylanase *NS50030* on the *Lfbsp* produced the
334 maximum amount of DP2 to DP6 oligosaccharides at 5 h of hydrolysis, equivalent to a
335 production yield of 88.0%. This yield is like that obtained in the *Maf* assay (88.4%),
336 though in the shortest time. This result may be because the enzyme endo-β-(1,4)-D-
337 xylanase *NS50030* also exhibits α-L-arabinofuranosidase activity (Nieto, 2017).

338 As in using pure enzymes, xylobiose and xylotriose were the majority XOS
339 generated after hydrolysis. The concentration of X_2 increased throughout enzymatic
340 hydrolysis until it reached a maximum concentration of 13.8 g/L, while the
341 concentrations of X_3, X_4, X_5, and X_6 decreased (Fig. 3a). It is also observed the increase
342 in X_3 production during the first two hours of EH. After this time, X_3 begins to decrease
343 in concentration, increasing the xylobiose concentration. The same commercial endo-β-
344 (1,4)-D-xylanase was used combined with arabinofuranosidase to obtain XOS from a
345 mixture of sugarcane bagasse and straw for Ávila et al., 2020a. Several pretreatments
346 (ionic liquid and dilute sulfuric acid) were studied in this work, being xylobiose the main
347 product in both pretreatments.

348 **Fig. 3**

349 The maximum amount of XOS achieved was 12.3 g (expressed as xylose)/100 g of
350 raw material, which was achieved at 5 h of hydrolysis. This same enzyme dose (7.2
351 U/mL) was used on pretreated wheat straw (Álvarez et al., 2017), reaching a value of 8.9
352 g XOS/100 g wheat straw. The lower yield obtained in wheat straw is mainly associated
353 with partial degradation of the hemicellulose fraction due to the high temperatures used
354 in the pretreatment (200 ºC).

About the release of xylose, glucose and arabinose, the amounts obtained represent 5.6%, 25.4% and 76.9%, respectively, of those potentially present, due to the action of the accessory activities *NS50030* enzymatic preparation.

3.2.4. Enzymatic hydrolysis using a commercial endo-β-(1,4)-D-xylanase, α-L-arabinofuranosidase, acetylxylan esterase and feruloyl esterase

Like the previous case, the aimed to study the behaviour of complementary enzymes (α-L-arabinofuranosidase, acetylxylan esterase and feruloyl esterase) with commercial endo-β-(1,4)-D-xylanase *NS50030* under the same conditions under which the previous assay was carried out. This cocktail enzymatic is called *NSAFA*.

The action of the enzyme acetylxylan esterase released a concentration of acetyl groups from the acetylated oligosaccharides, measured as acetic acid of 0.6 g/L, which is equivalent to 41.2% of the potential acetic acid (referred to the value measured after mild acid hydrolysis with sulfuric acid). This value is lower than expected; this could be because the hydrolysis conditions were not optimal for acetylxylan esterase in terms of pH conditions. The hydrolysis tests under conditions close to the optimum pH for the acetylxylan esterase enzyme resulted in a yield of more than 85% release of the acetyl groups.

The effect of incorporating feruloyl esterase enzyme in the hydrolysis medium with *NS50030* was a progressive release of *p*-coumaric and ferulic acids throughout the hydrolysis time. The highest concentration released was 100 mg/L of ferulic acids and 49 mg/L of *p*-coumaric. The release of these lignin derivatives did not result in an appreciable increase in arabinose to which (1→5) bonds link them.

377 Xylobiose was the majority XOS produced throughout commercial EH endo-β-
378 (1,4)-D-xylanase along with accessory enzymes (Fig. 2b). X_2 was increasing to a
379 concentration of 15.7 g/L at 6 h. Xylotriose concentration increased up to 1 h of
380 hydrolysis with a value of 7.3 g/L from which it decreased to values of 2.3 g/L at 6 h.
381 The remaining XOS of X_4, X_5 and X_6 were hydrolysed and transformed to xylotriose.
382 Despite the increase in xylobiose at 6 h, the highest concentration of XOS (DP2-DP6)
383 was produced at 3 h of hydrolysis, obtaining 12.1 g of XOS (DP 2-DP6) expressed as
384 xylose/ 100 g of barley straw. This value is similar to that obtained in the assay of
385 *NS50030* individually, which leads to the conclusion that, under the conditions studied,
386 the complementary enzymes α-L-arabinofuranosidase, acetylxylan esterase and feruloyl
387 esterase do not help the β-(1,4)-D-xylanase *NS50030* enzyme in the release of XOS with
388 (DP2-DP6).
389 Figure 4 shows the total concentration of XOS (DP2-DP6). The highest
390 concentrations of XOS (DP2-DP6) were released by *Complex* enzymatic hydrolysis.
391 This cocktail enzymatic produced 8.6 g/L of XOS in a short time (less than one hour).
392 At the same time, the other assays produced almost 1.5 g/L lower than the *Complex*
393 cocktail.
394 **Fig. 4**.
395 The literature showed a great deal of paper that used endoxylanase to produce
396 XOS from agriculture residues. Goldbeck et al. (2016) studied the effect of a mixture of
397 recombinant endoxylanase and a feruloyl esterase using sugar cane bagasse as raw
398 material. These authors achieved 356 mg of XOS/g xylan. This value is lower in
399 comparison with the results obtained in the assays carried out in this work (557; 588;
400 and 547 mg of XOS/g xylan in *Maf*; *Complex* and *NSAFA*, respectively). However, Liu

et al., (2018) evaluated XOS production in corn cobs using *Paenibacillus barengoltzii* xylanase. The yield obtained was 750 mg XOS /g xylan. Although this value is higher than obtained in this work, our enzymatic hydrolysis achieved XOS with a degree of polymerisation between DP2-DP6 since Liu obtained DP2-DP4. The use of endo-β-(1,4)-D-xylanase commercial and α-L-arabinofuranosidase in a sugarcane bagasse produced 338 mg of XOS/ g xylan extracted (Ávila et al., 2020b). In this case, the amount is smaller than achieved in our assays of EH.

Several feedstocks such as corncob, rice straw, and almond shells also were used for producing XOS. In these cases, in a range between 180-110 mg of XOS from g of biomass were obtained because of enzymatic hydrolysis using several enzymes and pretreatment (Han et al., 2020; Le and Yang, 2019; Singh et al., 2019). These studies suggest that accessory enzymes act synergistically with endo-β-(1,4)-D-xylanase enzyme during the EH of barley straw pretreated to produce the relevant products such as XOS. The difference of results between *Complex* assays and *NSAFA* is due to the mechanism of heterosynergism. In this case, the heterosynergism occurred for the initial activity of the main depolymerising endo-β-(1,4)-D-xylanase, which produce the substrate for the auxiliary enzyme.

3.3. PSSF process

The PSSF process was carried out with the WIS fraction at optimum conditions based on previous work (Álvarez et al., 2018). An ethanol concentration close to 50 g/L was obtained after 48 h, the ethanol yield was 22.3 g ethanol/g solid pretreated. Lara-Serrano et al. (2018) obtained similar yields in BS pretreated with ionic liquids (22.9 g/100 g pretreated straw).However, in this case, and given the type of pretreatment,

there has been no separation of the hemicellulose fraction to obtain xylooligosaccharides.

S. cerevisiae Ethanol Red, the yeast used, exclusively ferments the hexoses to ethanol so that all the xylose produced in the enzymatic hydrolysis stage can not be fermented to ethanol, leaving at the end of the process a final concentration in the fermentation medium around 4-6 g/L of xylose. This xylose could be fermented together with glucose if a co-fermentation strategy was used using microorganisms capable of fermenting both sugars, slightly increasing the final ethanol yield of the process. The overall ethanol production yield in this work was 12.6 g ethanol/100 g of BS, higher than that obtained by Duque et al. (2014), which reported overall yield values of 11.0 g ethanol/100 g of raw material using barley straw and a combined alkali and extrusion pretreatment. More recently, higher production (15.8 g ethanol/100 g of raw material) was reported from barley straw pretreated by combined alkaline and enzyme-catalysed extrusion in a simultaneous saccharification and co-fermentation process genetic modified S. *cerevisiae* strain (Duque et al., 2020). In this case, the hemicellulose fraction was also used for ethanol production.

Other authors also used a wheat straw has been submitted to produce XOS and bioethanol. For example, Huang et al. (2017) achieved similar cellulose conversion to ethanol at the present work (0.41 g ethanol/ g cellulose vs 0.42 g ethanol/ g cellulose). However, the fermentation time was less than 48 h in our study, obtaining higher volumetric productivities. Huang et al. (2017) achieved 229 mg of XOS per gram of xylan (mainly xylobiose and xylotriose) using endoxylanase. This value is less than obtained in this work.

3.4. Characterisation of lignin-rich residue

The chemical composition of the lignin-rich residue obtained after the PSSF process is depicted in figure 1. In this residue, the main component was lignin showing content of 74.5%, as expected. In the literature are described similar values for red maple (76%) or olive tree pruning (77%), or such lower as is switchgrass (59%) or wheat straw (69%) (Sannigrahi and Ragauskas, 2011; Santos et al., 2015). However, in the lignin-rich residue, a certain amount of cellulose and hemicellulose were quantified. The composition is carbon 54.1%, hydrogen 6.1% and nitrogen 2.4%. Given the high proportion of lignin in the residue and also its high heating value (23.4 MJ/kg, HHV dry basis) this residue proves a suitable green energy source or a precursor for lignin-based fuels and biomaterials. This lignin can be used in many applications such as energetic sources to improve the economy of the process.

The residue solid of lignin after simultaneous saccharification fermentation contains a high value of lignin. This residue has been characterised using FTIR spectroscopy (see the supplementary material).

A strong, wide band was shown in the spectrum, between 3500 and 3100 $cm^{-1.}$ These bands are assigned to OH stretching vibrations by the presence of alcoholic and phenolic hydroxyl groups involved in hydrogen bonds. The region between 2920 cm^{-1} and 2850 cm^{-1} is assigned to C H stretching vibrations in methyl and methylene groups. The intensity of bands 1510 cm^{-1} has contributed to aliphatic contribution, including carbohydrates and aliphatics side chains in lignin, concerning the aromatic part (Rossberg et al., 2015). In this spectrum, typical band attributed to polysaccharides such as at 1740 cm-1 the C=O stretching vibrations in the ester o carboxyl acid groups or 890 cm-1 β-Glycosidic linkages in pyranose were weak observed. The shoulders at 1719 cm^{-1} originate from unconjugated and carbonyl stretches.

Aromatic skeletal vibrations give three strong peaks at 1595, 1509 and 1419 cm^{-1} (Sun et al., 2011). These bands are the most characteristic vibrations of lignins (Nunes and Pardini, 2019). Other bands assigned were: 1458 cm^{-1} (asymmetric C–H deformations), 1356 cm^{-1} (symmetric C–H bending), 1319 cm^{-1} (syringyl ring breathing with C–O stretching), 1265 cm^{-1} shoulder (guaiacyl ring breathing with C O stretching), 1090 cm^{-1} (C–O deformation, secondary alcohol and aliphatic ethers), 1030 cm^{-1} (aromatic C–H in-plane deformation plus C–O in primary alcohols, guaiacyl type), 1321 cm^{-1} (symmetric C–H bending), 1265 cm^{-1} shoulder (guaiacyl ring breathing with C O stretching), 1086 cm^{-1} (C–O deformation, secondary alcohol and aliphatic ethers).

The spectra have a stronger wide band at 1030 cm^{-1} than that band at 1136 cm^{-1} indicate the content of the guaiacyl (G) unit is higher than that of the syringyl (S) unit with high condensation (Sun et al., 2011). Also, the band at 901 cm^{-1} indicated aromatic C–H out-of-plane bending in G units, whereas the band at 823 cm^{-1} represented C–H out-of-plane bending in positions 2 and 6 of S units and all positions of *p*-hydroxyphenyl units

These results and the high lignin content in this residue offer the possibility of valorisation of this residue in a biorefinery concept. However, its necessary further studies in order to evaluate the actual potential of the utilisation of this residue since it has been described that SE produce a higher abundance of β-O-4’ linkages compared to industrial lignin (Santos et al., 2015). Lignin-rich residue can be transformed into high added value products such as building blocks for materials and fuels.

3.5. Overall process material balance

The diagram integrates the process of obtaining XOS (DP2-DP6) and bioethanol from liquid and solid fractions, respectively, in figure 5. In the context of a biorefinery

process to valorisation, the barley straw residue is proposed to carry out a steam explosion such as pretreatment, with the object to alter the structure. Concerning pretreatment (180 ºC 30 min), these conditions allowed an excellent recovery of hemicellulose and cellulose in liquid fraction and solid fraction.

This paper has been a detailed process for obtaining XOS with a degree of polymerisation DP2-DP6 from liquid fraction of barley straw pretreated through enzymatic hydrolysis. 13.0 g of XOS per 100 g of raw material have been achieved using the *Complex* cocktail enzymatic. After pretreatment, 54.1 g solid was recovered, including 30.2 g of glucan, 5.6 g xylan and practically all lignin (16.7 g). High ethanol yield from solid fraction was achieved using presaccharification and simultaneous fermentation with high solid concentration (20% w/v). The final residue contained un-hydrolysed cellulose and xylan fermentation and a high amount of lignin, which have been characterised using FTIR technique (previous section).

The result indicated that BS could be used to obtain bioproducts such as bioethanol, XOS, and a lignin-rich residue to revalue an agriculture residue.

Fig. 5

4. Conclusions

BS is a potential raw material to obtain bioethanol and value-added products such as xylooligosaccharides for application in diverse industries. The strategy followed in this study for obtained XOS was pretreated the raw material with SE following EH through endo-β-(1,4)-D-xylanase and accessory enzymes were tested. The increment production of XOS (DP2-DP6) with respect to liquid fraction of barley straw pretreated was in the system *Maf, Complex*, commercial endo-β-(1,4)-D-xylanase, *NSAFA* was 56%, 64%, 55% and 53% respectively. Integration of bioethanol and bioproducts from

raw material could improve the economy of a possible biorefinery.

Acknowledgements

The authors thank you for the financial support of the Comunidad de Madrid-CM (Spain) (Project RESTOENE-2-CM,S2013/MAE-2882).

Reference

1. Ahuja, Mamtani, 2021. Prebiotics market size by ingredients (Fructo-oligosaccharide (FOS), Inulin, Galacto-oligosaccharides (GOS), Mannan-oligosaccharide (MOS)), By application (prebiotic food & beverages {dairy products, cereals, baked food, fermented meat products, dry food [WWW Document]. URL https://www.gminsights.com/industry-analysis/prebiotics-market
2. Álvarez, C., González, A., Alonso, J.L., Sáez, F., Negro, M.J., Gullón, B., 2020. Xylooligosaccharides from steam-exploded barley straw : Structural features and assessment of bifidogenic properties. Food Bioprod. Process. 124, 131–142. https://doi.org/10.1016/j.fbp.2020.08.014
3. Álvarez, C., González, A., Negro, M.J., Ballesteros, I., Oliva, J.M., Sáez, F., 2017. Optimized use of hemicellulose within a biorefinery for processing high value-added xylooligosaccharides. Ind. Crops Prod. 99, 41–48. https://doi.org/10.1016/j.indcrop.2017.01.034
4. Álvarez, C., Sáez, F., González, A., Ballesteros, I., Oliva, J.M., Negro, M.J., 2018. Production of xylooligosaccharides and cellulosic ethanol from steam-exploded barley straw. Holzforschung 73, 35–44. https://doi.org/10.1515/hf-2018-0101
5. Arai, T., Biely, P., Uhliariková, I., Sato, N., Makishima, S., Mizuno, M., Nozaki, K., Kaneko, S., Amano, Y., 2019. Structural characterization of hemicellulose released from corn cob in continuous flow type hydrothermal reactor. J. Biosci. Bioeng. 127, 222–230. https://doi.org/10.1016/j.jbiosc.2018.07.016
6. Ávila, P.F., Franco Cairo, J.P.L., Damasio, A., Forte, M.B.S., Goldbeck, R., 2020a. Xylooligosaccharides production from a sugarcane biomass mixture: Effects of commercial enzyme combinations on bagasse/straw hydrolysis pretreated using different strategies. Food Res. Int. 128, 108702. https://doi.org/10.1016/j.foodres.2019.108702
7. Ávila, P.F., Martins, M., de Almeida Costa, F.A., Goldbeck, R., 2020b.

551 Xylooligosaccharides production by commercial enzyme mixture from agricultural wastes and
552 their prebiotic and antioxidant potential. Bioact. Carbohydrates Diet. Fibre 24, 1–9.
553 https://doi.org/10.1016/j.bcdf.2020.100234
554 8. Biely, P., Cziszárová, M., Uhliariková, I., Agger, J.W., Li, X.L., Eijsink, V.G.H.,
555 Westereng, B., 2013. Mode of action of acetylxylan esterases on acetyl glucuronoxylan and
556 acetylated oligosaccharides generated by a GH10 endoxylanase. Biochim. Biophys. Acta -
557 Gen. Subj. 1830, 5075–5086. https://doi.org/10.1016/j.bbagen.2013.07.018
558 9. Biely, P., Singh, S., Puchart, V., 2016. Towards enzymatic breakdown of complex plant
559 xylan structures: State of the art. Biotechnol. Adv. 34, 1260–1274.
560 https://doi.org/10.1016/j.biotechadv.2016.09.001
561 10. Brienzo, M., Carvalho, A.F.A., de Figueiredo, F.C., de Oliva Neto, P., 2016. Sugarcane
562 bagasse hemicellulose properties, extraction technologies and xylooligosaccharides production,
563 Food waste: Practices, Management and Challenges. Nova Science Publisher, Inc, New York,
564 NY.
565 11. de Oliveira, D.M., Finger-Teixeira, A., Rodrigues Mota, T., Salvador, V.H., Moreira-Vilar,
566 F.C., Correa Molinari, H.B., Craig Mitchell, R.A., Marchiosi, R., Ferrarese-Filho, O., Dantas
567 dos Santos, W., 2015. Ferulic acid: A key component in grass lignocellulose recalcitrance to
568 hydrolysis. Plant Biotechnol. J. 13, 1224–1232. https://doi.org/10.1111/pbi.12292
569 12. Duque, A., Doménech, P., Álvarez, C., Ballesteros, M., Manzanares, P., 2020. Study of the
570 bioprocess conditions to produce bioethanol from barley straw pretreated by combined soda
571 and enzyme-catalyzed extrusion. Renew. Energy 158, 263–270.
572 https://doi.org/10.1016/j.renene.2020.05.130
573 13. Duque, A., Manzanares, P., Ballesteros, I., Ballesteros, M., 2016. Steam explosion as
574 lignocellulosic biomass pretreatment, in: Mussatto, S.I. (Ed.), Biomass Fractionation
575 Technologies for a Lignocellulosic Feedstock Based Biorefinery. Amsterdam, The
576 Netherlands, pp. 349–368. https://doi.org/10.1016/B978-0-12-802323-5.00015-3

14. Duque, A., Manzanares, P., Ballesteros, I., Negro, M.J., Oliva, J.M., González, A., Ballesteros, M., 2014a. Sugar production from barley straw biomass pretreated by combined alkali and enzymatic extrusion. Bioresour. Technol. 158, 262–268. https://doi.org/10.1016/j.biortech.2014.02.041

15. Duque, A., Manzanares, P., Ballesteros, I., Negro, M.J., Oliva, J.M., Saez, F., Ballesteros, M., 2014b. Study of process configuration and catalyst concentration in integrated alkaline extrusion of barley straw for bioethanol production. Fuel 134, 448–454. https://doi.org/10.1016/j.fuel.2014.05.084

16. Fernández, J., Redondo-Blanco, S., Gutiérrez-del-Río, I., Miguélez, E.M., Villar, C.J., Lombó, F., 2016. Colon microbiota fermentation of dietary prebiotics towards short-chain fatty acids and their roles as anti-inflammatory and antitumour agents: A review. J. Funct. Foods 25, 511–522. https://doi.org/10.1016/j.jff.2016.06.032

17. Gibson, G.R., Hutkins, R., Sanders, M.E., Prescott, S.L., Reimer, R.A., Salminen, S.J., Scott, K., Stanton, C., Swanson, K.S., Cani, P.D., Verbeke, K., Reid, G., 2017. Expert consensus document: The International Scientific Association for Probiotics and Prebiotics (ISAPP) consensus statement on the definition and scope of prebiotics. Nat. Rev. Gastroenterol. Hepatol. 14, 491–502. https://doi.org/10.1038/nrgastro.2017.75

18. Gírio, F.M., Fonseca, C., Carvalheiro, F., Duarte, L.C., Marques, S., Bogel-Łukasik, R., 2010. Hemicelluloses for fuel ethanol: A review. Bioresour. Technol. 101, 4775–4800. https://doi.org/10.1016/j.biortech.2010.01.088

19. Goldbeck, R., Gonçalves, T.A., Damásio, A.R.L., Brenelli, L.B., Wolf, L.D., Paixão, D.A.A., Rocha, G.J.M., Squina, F.M., 2016. Effect of hemicellulolytic enzymes to improve sugarcane bagasse saccharification and xylooligosaccharides production. J. Mol. Catal. B Enzym. 131, 36–46. https://doi.org/10.1016/j.molcatb.2016.05.013

20. Gullón, B., Eibes, G., Dávila, I., Moreira, M.T., Labidi, J., Gullón, P., 2018. Hydrothermal treatment of chestnut shells (*Castanea sativa*) to produce oligosaccharides and antioxidant

603 compounds. Carbohydr. Polym. 192, 75–83. https://doi.org/10.1016/j.carbpol.2018.03.051
604 21. Han, J., Cao, R., Zhou, X., Xu, Y., 2020. An integrated biorefinery process for adding
605 values to corncob in co-production of xylooligosaccharides and glucose starting from
606 pretreatment with gluconic acid. Bioresour. Technol. 307, 123200.
607 https://doi.org/10.1016/j.biortech.2020.123200
608 22. Houfani, A.A., Anders, N., Spiess, A.C., Baldrian, P., Benallaoua, S., 2020. Insights from
609 enzymatic degradation of cellulose and hemicellulose to fermentable sugars– a review.
610 Biomass and Bioenergy 134, 105481. https://doi.org/10.1016/j.biombioe.2020.105481
611 23. Huang, C., Lai, C., Wu, X., Huang, Y., He, J., Huang, Caoxing, Li, X., Yong, Q., 2017. An
612 integrated process to produce bio-ethanol and xylooligosaccharides rich in xylobiose and
613 xylotriose from high ash content waste wheat straw. Bioresour. Technol. 241, 228–235.
614 https://doi.org/10.1016/j.biortech.2017.05.109
615 24. Lara-Serrano, M., Sáez Angulo, F., Negro, M.J., Morales-Delarosa, S., Campos-Martin,
616 J.M., Fierro, J.L.G., 2018. Second-Generation bioethanol production combining simultaneous
617 fermentation and saccharification of IL-pretreated barley straw. ACS Sustain. Chem. Eng. 6,
618 7086–7095. https://doi.org/10.1021/acssuschemeng.8b00953
619 25. Le, B., Yang, S.H., 2019. Production of prebiotic xylooligosaccharide from aqueous
620 ammonia-pretreated rice straw by β-xylosidase of *Weissella cibaria*. J. Appl. Microbiol. 126,
621 1861–1868. https://doi.org/10.1111/jam.14255
622 26. Limayem, A., Ricke, S.C., 2012. Lignocellulosic biomass for bioethanol production:
623 Current perspectives, potential issues and future prospects. Prog. Energy Combust. Sci. 38,
624 449–467. https://doi.org/10.1016/j.pecs.2012.03.002
625 27. Liu, X., Liu, Y., Jiang, Z., Liu, H., Yang, S., Yan, Q., 2018. Biochemical characterization of
626 a novel xylanase from Paenibacillus barengoltzii and its application in xylooligosaccharides
627 production from corncobs. Food Chem. 264, 310–318.
628 https://doi.org/10.1016/j.foodchem.2018.05.023

28. Moreno, A.D., Tomás-Pejó, E., Ballesteros, M., Negro, M.J., 2019. Pretreatment technologies for lignocellulosic biomass deconstruction within a biorefinery perspective, in: Pandey, A., Larroche, C., Dussap, C.-G., Gnansounou, E., Khanal, S.K., Ricke, S.C. (Eds.), Biofuels: Alternative Feedstocks and Conversion Processes for the Production of Liquid and Gaseous Biofuels. Amsterdam, The Netherlands, pp. 379–399. https://doi.org/10.1016/c2018-0-00957-3

29. Negro, M.J., Alvarez, C., Ballesteros, I., Romero, I., Ballesteros, M., Castro, E., Manzanares, P., Moya, M., Oliva, J.M., 2014. Ethanol production from glucose and xylose obtained from steam exploded water-extracted olive tree pruning using phosphoric acid as catalyst. Bioresour. Technol. 153, 101–107. https://doi.org/10.1016/j.biortech.2013.11.079

30. Nieto, M., 2017. Study of fungal xylanases for the exploitation of lignocellulosic biomass. UCM.

31. Nunes, K., Pardini, L., 2019. Purification and characterization methods for lignin biomass as a potnential precursor for carbon materials. Cellul. Chem. Technol. 53, 227–242. https://doi.org/10.35812/CelluloseChemTechnol.2019.53.23

32. Pinales-Márquez, C.D., Rodríguez-Jasso, R.M., Araújo, R.G., Loredo-Treviño, A., Nabarlatz, D., Gullón, B., Ruiz, H.A., 2021. Circular bioeconomy and integrated biorefinery in the production of xylooligosaccharides from lignocellulosic biomass: A review. Ind. Crops Prod. 162. https://doi.org/10.1016/j.indcrop.2021.113274

33. Reddy, S.S., Krishnan, C., 2016. Production of high-pure xylooligosaccharides from sugarcane bagasse using crude β-xylosidase-free xylanase of Bacillus subtilis KCX006 and their bifidogenic function. LWT - Food Sci. Technol. 65, 237–245. https://doi.org/10.1016/j.lwt.2015.08.013

34. Rico, X., Gullón, B., Alonso, J.L., Parajó, J.C., Yáñez, R., 2018. Valorization of *peanut shells*: Manufacture of bioactive oligosaccharides. Carbohydr. Polym. 183, 21–28. https://doi.org/10.1016/j.carbpol.2017.11.009

655 35. Rossberg, C., Bremer, M., Machill, S., Koenig, S., Kerns, G., Boeriu, C., Windeisen, E.,
656 Fischer, S., 2015. Separation and characterisation of sulphur-free lignin from different
657 agricultural residues. Ind. Crops Prod. 73, 81–89.
658 https://doi.org/10.1016/j.indcrop.2015.04.001
659 36. Sadaf, A., Khare, S.K., 2014. Production of *Sporotrichum thermophile* xylanase by solid
660 state fermentation utilizing deoiled *Jatropha curcas* seed cake and its application in
661 xylooligosaccharide synthesis. Bioresour. Technol. 153, 126–130.
662 https://doi.org/10.1016/j.biortech.2013.11.058
663 37. Sáez, F., Ballesteros, M., Ballesteros, I., Manzanares, P., Oliva, J.M., Negro, M.J., 2013.
664 Enzymatic hydrolysis from carbohydrates of barley straw pretreated by ionic liquids. J. Chem.
665 Technol. Biotechnol. 88, 937–941. https://doi.org/10.1002/jctb.3925
666 38. Sannigrahi, P., Ragauskas, A.J., 2011. Characterization of fermentation residues from the
667 production of bio-ethanol from lignocellulosic feedstocks. J. Biobased Mater. Bioenergy 5,
668 514–519. https://doi.org/10.1166/jbmb.2011.1170
669 39. Santos, J.I., Martín-Sampedro, R., Fillat, Ú., Oliva, J.M., Negro, M.J., Ballesteros, M.,
670 Eugenio, M.E., Ibarra, D., 2015. Evaluating lignin-rich residues from biochemical ethanol
671 production of wheat straw and olive tree pruning by FTIR and 2d-nmr. Int. J. Polym. Sci. 2015.
672 https://doi.org/10.1155/2015/314891
673 40. Singh, R.D., Nadar, C.G., Muir, J., Arora, A., 2019. Green and clean process to obtain low
674 degree of polymerisation xylooligosaccharides from *almond shell*. J. Clean. Prod. 241, 118237.
675 https://doi.org/10.1016/j.jclepro.2019.118237
676 41. Slavin, J., 2013. Fiber and prebiotics: Mechanisms and health benefits. Nutrients 5, 1417–
677 1435. https://doi.org/10.3390/nu5041417
678 42. Sluiter, J.B., Ruiz, R.O., Scarlata, C.J., Sluiter, A.D., Templeton, D.W., 2010.
679 Compositional analysis of lignocellulosic feedstocks. 1. Review and description of methods. J.
680 Agric. Food Chem. 58, 9043–9053. https://doi.org/10.1021/jf1008023

681 43. Sun, X.F., Jing, Z., Fowler, P., Wu, Y., Rajaratnam, M., 2011. Structural characterization
682 and isolation of lignin and hemicelluloses from barley straw. Ind. Crops Prod. 33, 588–598.
683 https://doi.org/10.1016/j.indcrop.2010.12.005
684 44. Vazquez-Olivo, G., Gutiérrez-Grijalva, E.P., Heredia, J.B., 2019. Prebiotic compounds from
685 agro-industrial by-products. J. Food Biochem. 43, 1–8. https://doi.org/10.1111/jfbc.12711
686 45. Wietschel, L., Thorenz, A., Tuma, A., 2019. Spatially explicit forecast of feedstock
687 potentials for second generation bioconversion industry from the EU agricultural sector until
688 the year 2030. J. Clean. Prod. 209, 1533–1544. https://doi.org/10.1016/j.jclepro.2018.11.072
689 46. Wong, D.W.S., Chan, V.J., Liao, H., Zidwick, M.J., 2013. Cloning of a novel feruloyl
690 esterase gene from rumen microbial metagenome and enzyme characterization in synergism
691 with endoxylanases. J. Ind. Microbiol. Biotechnol. 40, 287–295.
692 https://doi.org/10.1007/s10295-013-1234-1
693 47. Wu, H., Li, H., Xue, Y., Luo, G., Gan, L., Liu, J., Mao, L., Long, M., 2017. High efficiency
694 co-production of ferulic acid and xylooligosaccharides from wheat bran by recombinant
695 xylanase and feruloyl esterase. Biochem. Eng. J. 120, 41–48.
696 https://doi.org/10.1016/j.bej.2017.01.001
697 48. Zhang, J., Siika-Aho, M., Tenkanen, M., Viikari, L., 2011. The role of acetyl xylan esterase
698 in the solubilization of xylan and enzymatic hydrolysis of wheat straw and giant reed.
699 Biotechnol. Biofuels 4. https://doi.org/10.1186/1754-6834-4-60
700 49. Zhang, W., You, Y., Lei, F., Li, P., Jiang, J., 2018. Acetyl-assisted autohydrolysis of
701 sugarcane bagasse for the production of xylo-oligosaccharides without additional chemicals.
702 Bioresour. Technol. 265, 387–393. https://doi.org/10.1016/j.biortech.2018.06.039
703 50. Zheng, F., Huang, J., Yin, Y., Ding, S., 2013. A novel neutral xylanase with high SDS
704 resistance from Volvariella volvacea: Characterization and its synergistic hydrolysis of wheat
705 bran with acetyl xylan esterase. J. Ind. Microbiol. Biotechnol. 40, 1083–1093.
706 https://doi.org/10.1007/s10295-013-1312-4

List of figures

718

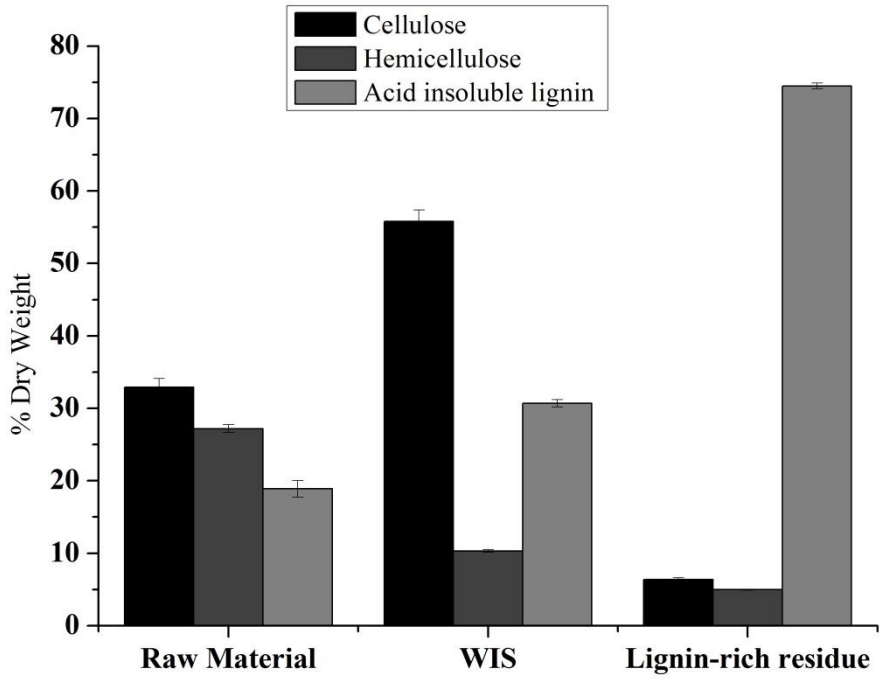

719

720 **Figure** 1.

721

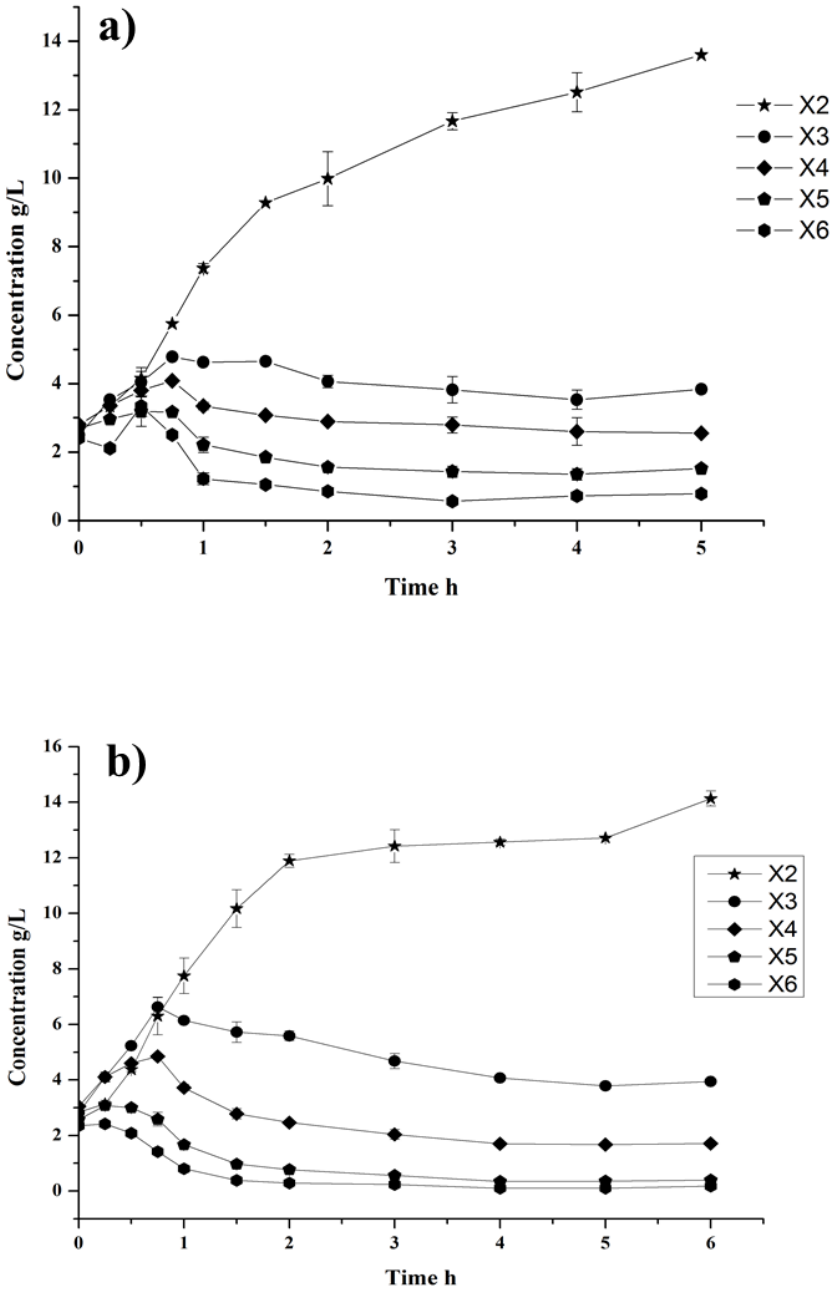

722

723 **Figure 2.**

724

725

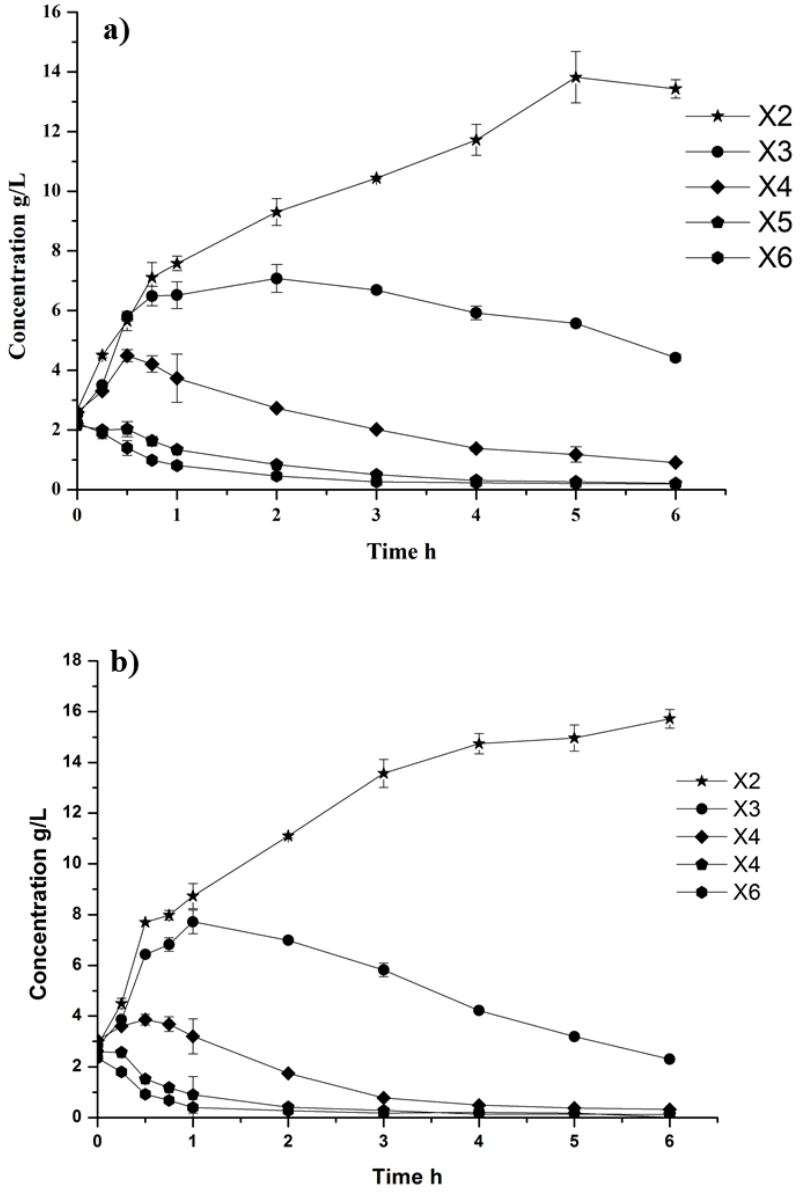

726

727 **Figure 3**:

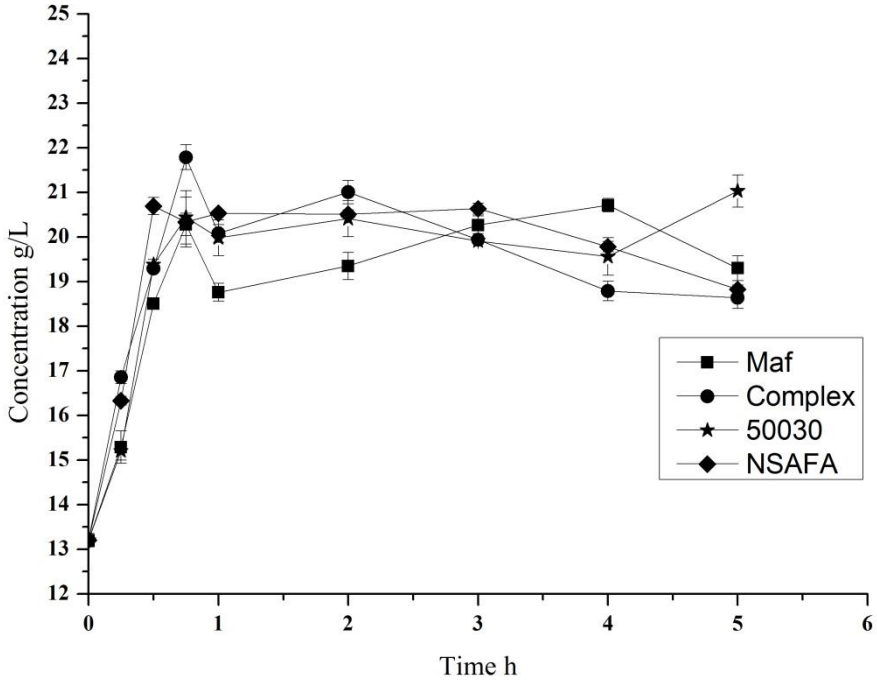

728

729 **Figure 4**.

730

731

732

733

734

735

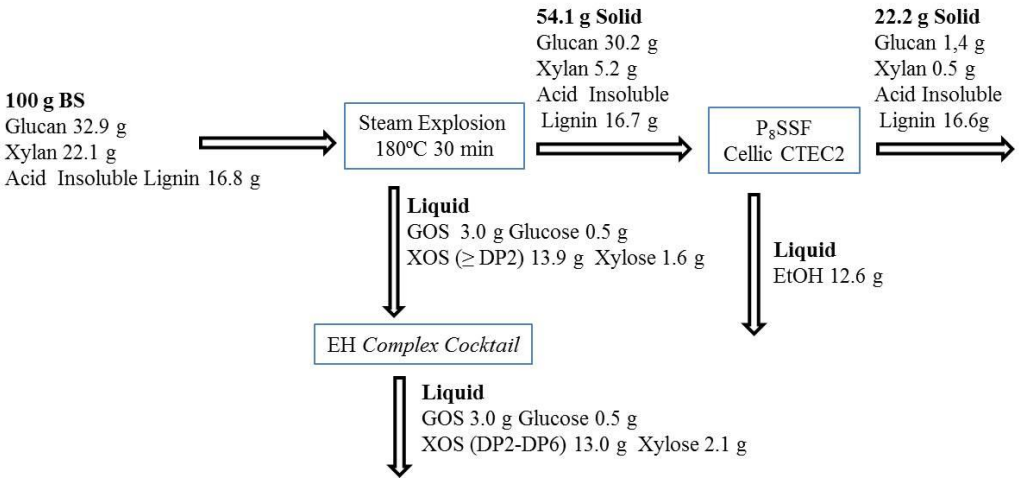

736

737 Figure 5

738

739

740